



**HAL**  
open science

## Parallelization of Dielectric Measurements at Microwaves for Microfluidic Biosensor Arrays

M Schüßler, M Puentes, R Jakoby, David Dubuc, Katia Grenier

► **To cite this version:**

M Schüßler, M Puentes, R Jakoby, David Dubuc, Katia Grenier. Parallelization of Dielectric Measurements at Microwaves for Microfluidic Biosensor Arrays. IEEE European Microwave Conference, Sep 2015, Paris, France. pp.833-836, 10.1109/EuMC.2015.7345893 . hal-01951652

**HAL Id: hal-01951652**

**<https://laas.hal.science/hal-01951652>**

Submitted on 11 Jul 2022

**HAL** is a multi-disciplinary open access archive for the deposit and dissemination of scientific research documents, whether they are published or not. The documents may come from teaching and research institutions in France or abroad, or from public or private research centers.

L'archive ouverte pluridisciplinaire **HAL**, est destinée au dépôt et à la diffusion de documents scientifiques de niveau recherche, publiés ou non, émanant des établissements d'enseignement et de recherche français ou étrangers, des laboratoires publics ou privés.

# Parallelization of Dielectric Measurements at Microwaves for Microfluidic Biosensor Arrays

M. Schüßler, M. Puentes, R. Jakoby

Institute of Microwave Engineering and Photonics,  
TU Darmstadt, Merckstrasse 25,  
D-64283 Darmstadt, Germany  
schuessler@imp.tu-darmstadt.de

D. Dubuc, K. Grenier

Fluidic High Frequency Micro and Nanosystems Group  
LAAS-CNRS, 7, avenue du Colonel Roche  
31077 Toulouse Cedex 4, France

**Abstract**— An approach for the parallelization of dielectric measurements at microwaves within a lab-on-a-chip environment is presented. Its targeted application is the simultaneous monitoring of a cell suspension in microfluidic channel arrays under the influence of different drugs e.g. for an effectiveness assessment. The method has the advantage that only a single network analyzer and no other microwave components like switches or multiplexers are necessary. The paper presents the concept of the measurement system, prototype sensors, and their characterization. The realized devices operate between 20 and 25 GHz and have been tested with water, water-ethanol mixtures and Chinese Hamster Ovary (CHO) cells.

**Keywords**— Microwave, biosensor, biological cell, dielectric spectroscopy.

## I. INTRODUCTION

Impedance/dielectric spectroscopy has been proven to be a powerful tool for the analysis of biological substances because it allows for contact-less, marker-less and non-destructive/non-invasive measurements and real-time monitoring ability. The applications cover a wide field, a large frequency range from DC to lightwaves, and work with samples from macroscopic tissues down to single cells or even molecules [1-4].

In this context biosensors for the microwave regime using microfluidic technology for the analysis of cell suspensions and individual cells have recently been subject of intense research [5, 6], since they prospect new features compared with the devices operating at lower frequencies: first, the cells can be directly measured in their culture medium without any screening or measurement perturbation due to the ionic content of the biological medium, as the major ionic impact occurs below 1 GHz, and second, the waves may penetrate the cells and thus allow an improved insight [7, 8]. In the MHz frequency range the cells behave electromagnetically as a capacitive membrane with a conductive cytoplasm. As a perspective with increasing frequency up to the GHz domain the waves may overpass the capacitive bi-lipid membrane and interact with the interior constituents of the cell.

However, a drawback coming with microwaves is the necessity of elaborate and costly equipment. This point gets more important when it comes to the parallelizing of tests since the measurement hardware cannot be easily duplicated due to economical reasons. In contrast to many sensors that

allow the broadband characterization of the liquid in one channel [5, 6], this concept aims for the simultaneous narrowband monitoring of the dielectric constant in several channels with only one network analyzer. Although, demonstrated for the microwave regime, the sensor principle is extendable to mm-wave and lower THz bands.

## II. MEASUREMENT SYSTEM

The block diagram of the sensor system is depicted in Fig. 1. An electrical circuit is detuned in dependence of the filling of microfluidic channels. The electrical characteristic is measured with a vector network analyzer. The measured scattering parameters are subsequently processed with the goal to reduce the data and to extract characteristic features such as poles and zeros of the input impedance. In a final processing step the dielectric properties of the materials in the microfluidic channels are determined.

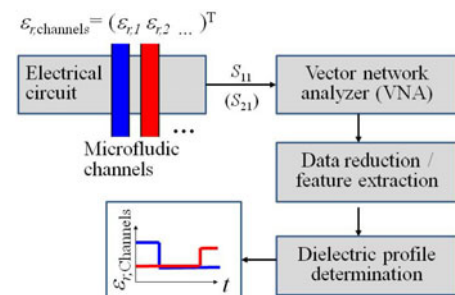


Fig. 1. Block diagram of the measurement system.

Basically, there exist an infinite number of implementations for the circuit part of the sensor from Fig. 1. An obvious approach would be to couple every channel with an electrical resonator and, hence, realize a frequency discrimination for the readout of the channels. However, because of space restrictions on a lab-on-a-chip, electromagnetic coupling effects, and poor quality factors of the resonators, this approach is not feasible. For this work a so called composite right/left-handed transmission line (CRLH TL) topology has been chosen for the electrical circuit as described in [9]. It offers various advantages: a straightforward design procedure because of the well known theoretical background, the realizability of the circuit in coplanar waveguide technology and the concept for data extraction that has already been demonstrated for this and

other applications [9-11]. The realized sensors are depicted in Fig. 2a. On the left side of the picture a device with a mounted channel is shown - on the right side circuits for devices with two channels and four channels. The equivalent circuit of the unit cell, as it is well known from CRLH TL theory, is depicted in Fig. 2b. As a proof that the electrical behavior of the sensor circuit can be described with cascaded unit cells, the fitting of S-Parameters for a four channel sensor has been done. The results are depicted in Fig. 2c for the following elements:  $L_R = 0.07$  nH,  $C_L = 0.16$  pF (0.18 pF with water),  $L_L = 0.10$  nH,  $C_R = 0.01$  nH. These parameters are used for further system consideration in section IV. The figure also shows the frequency band of operation for the sensor which covers the range between 20 and 25 GHz. Also the sensor works in a frequency band, the values for the extracted values of the relative dielectric constants are determined for 20 GHz. A broadband characterization of a liquid under test is not possible with this approach. The dispersion in the frequency band of operation is currently not considered by the method and increases the extraction error. Values for this extraction error for a four-channel device are presented in section IV.

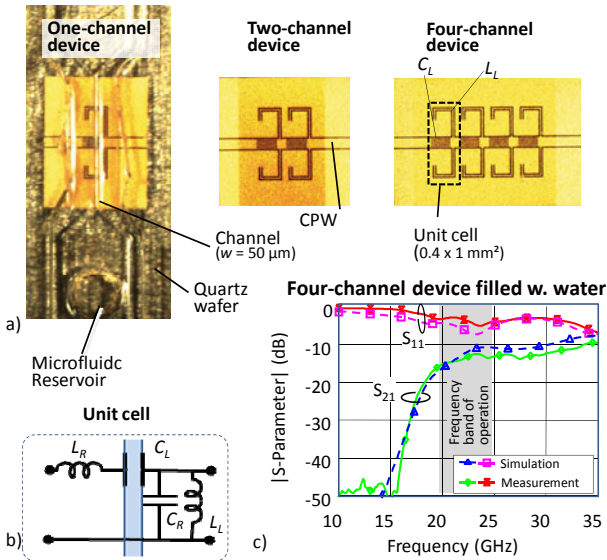


Fig. 2. a) Overview of the realized circuits for the prototypes. For the sensor on the left side the microfluidic channel has already been mounted. b) Equivalent circuit of a sensor circuit unit cell and c) fitted and measured S-parameters of a water filled four-channel sensor.

### III. DATA PROCESSING

The determination of the unknown material properties in the microfluidic channels is done in several steps. Initially, the scattering parameters of the circuit are transformed to impedance values and then the data volume is reduced by the extraction of the pole and zero information of the input impedance. Pole and zero information is used as the characteristic feature for the determination of the loading of the channels in a similar way as described in [10]:

$$\omega_{pz} = \mathbf{A} \cdot \boldsymbol{\varepsilon}_{r,\text{channel}} \quad (1)$$

where  $\omega_{pz}$  and  $\boldsymbol{\varepsilon}_{r,\text{channel}}$  are the vectors of the poles and zeros of the input impedance and of the relative dielectric constant of the liquid in the channels, respectively. The matrix  $\mathbf{A}$  is determined with tailored calibration measurements. These measurements are done with known liquids (water as a reference and water-ethanol mixtures for calibration with relative dielectric constants of  $\varepsilon_{r,REF}$  and  $\varepsilon_{r,CAL}$ , respectively) and defined loading situations, as explained in the following section. After the extraction of the poles and zeros information,  $\mathbf{A}$  is determined by solving a linear system of equations. For an unknown loading situation of the channels,  $\boldsymbol{\varepsilon}_{r,\text{channel}}$  can be calculated according to (1) by multiplication of  $\mathbf{A}^{-1}$  with  $\omega_{pz}$ . During some experiments common mode drift on the extracted data was observed, In this case it might be beneficial to use the differential formulation of (1) to determine  $\boldsymbol{\varepsilon}_{r,\text{channels}}$ :

$$\Delta\omega_{pz} = \mathbf{A} \cdot \Delta\boldsymbol{\varepsilon}_{r,\text{channel}} \quad (2)$$

The  $\Delta$ -operator refers to the difference of two subsequent measurements.

### IV. SYSTEM PERFORMANCE

Since (1) is only the linearization of a complex non-linear relationship between  $\omega_{pz}$  and  $\boldsymbol{\varepsilon}_{r,\text{channel}}$  calculations have been done in order to estimate the resulting error and the usable working range for the sensor.

Figure 3 shows the simulated performance of a four-channel sensor based on the sensor model from section II. Plotted are only the results for channel 1 and 2, since channels 3 and 4 behave in a similar way. The lines correspond to the imprinted dielectric loading situation in the channels and the symbols to the extracted values using (1). Measurements 1-5 are used for calibration purposes. Calibration is done in the following way: In measurement 1 all channels are filled with the reference liquid, in this work: water. In measurements 2-5 one channel at a time is successively filled with the calibration liquid. With this measurements  $\mathbf{A}$  can be determined as described in [10]. For the labeling of these liquids an “m” followed by the volumetric amount of ethanol has been used e.g. for the shown example *m20* stands for a mixture with 80% water and 20% ethanol volumetric content with  $\varepsilon_{r,CAL} = 19.7$  @20GHz. An overview of used liquids is provided in Table 1.

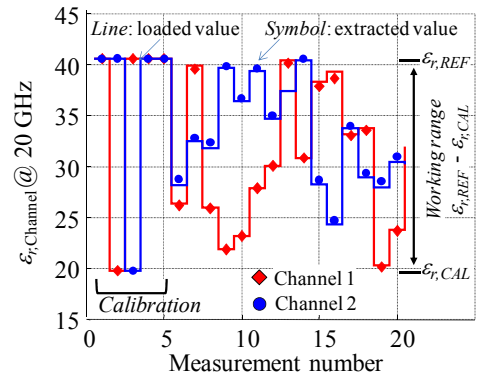


Fig. 3. Simulated sensor performance proofing the functioning of the extraction method. The reference liquid is water and the liquid used for calibration is *m20* (see Tab. 1). Channel 3 and 4 show similar behavior.

Starting from measurement 6 all four channels are simultaneously loaded with a random dielectric value in the working range of the sensor. The working range is defined in this paper as the interval from  $\epsilon_{r,CAL}$  to  $\epsilon_{r,REF}$ . Fig 3 shows exemplarily the results of the extraction procedure for 15 simulated loading situations with random loading of the channels. In summary the extraction follows the imprinted dielectric patterns, however, there are small errors visible, originating from the linearization used in (1) and the dispersive nature of the liquids.

TABLE I. USED LIQUIDS

Name	Ethanol (%)	Water (%)	$\epsilon_r$ @20GHz
Water	0	100	40.6
m5	5	95	34.0
m10	10	90	28.4
m15	15	85	24.0
m20	20	80	19.7
m50	50	50	12.1
Ethanol	100	0	4.9

An overview of the maximum observed extraction error of  $\epsilon_r$  is depicted in Fig. 4. The error is determined based on 200 simulated random loading profiles. For the graph the liquid used for the calibration has been varied. Obviously the error corresponds with the content of ethanol in the calibration liquid. The ethanol content is correlated with the working range of the sensor and, hence, the larger working range, the higher is the maximal error. Additionally, it should be noted that the error distribution in the channels is the same and channel 2 has the lowest error.

The question how many channels can be simultaneously monitored with this technique depends strongly on the specific application, since it will define the required extraction accuracy. The accuracy/extraction error depends on different system parameters e.g. the width of the frequency band the sensor requires for operation, the dispersive properties of liquids under test, the required resolution, the performance of the RF hardware (network analyzer) and so on. Additionally there is the possibility to reduce the extraction error by considering the dispersive properties of the used liquids and

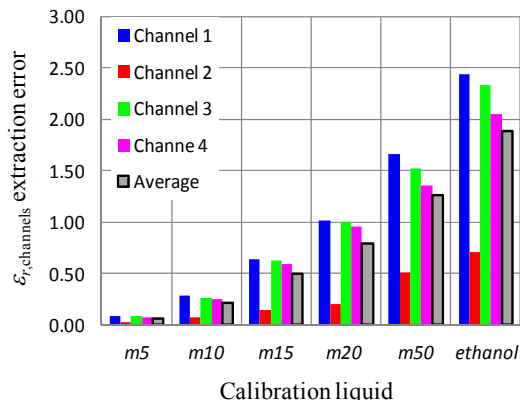


Fig. 4. Maximal extraction error for different calibration liquids.

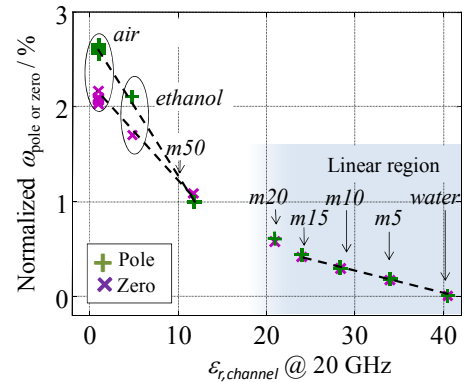


Fig. 5. The normalized frequencies for pole and zero of a one-channel device are plotted versus the relative dielectric constant  $\epsilon_{r,channel}$  of the material in the channel. The characteristic curve reveals the linear region where  $\omega_{pz} \sim \epsilon_{r,channel}$  and equations (1) and (2) can be applied.

by applying standard signal processing techniques. Currently there is only simulated data for the performance of a multi-channel sensor available. Hence, it is too early to give well-grounded prognosis for performance of such a system, particularly the number of simultaneously monitorable channels.

## V. EXPERIMENTAL RESULTS

Fig. 5 shows the results from the measurements of a one-channel device as depicted in Fig. 2a. In the plot, the relative shift in the frequency of the pole and the zero of the input impedance is plotted versus the relative dielectric constant of the material in the channel  $\epsilon_{r,channel}$ . The frequency of the pole and zero has been normalized to the scenario when the channel filled with water. Different loading situations have been realized with water-ethanol mixtures. The plot shows the validity for the assumption of linearity from water down to *m15*. In the simulations the resulting errors for  $\epsilon_{r,channel}$  determination is estimated to values of 0.6 and 0.25 when calibrating with *m15* and *m10*, respectively (see Fig. 4).

Fig. 6 shows an example for the operation of the sensor for varying loading conditions using living Chinese Hamster Ovary (CHO) cells, which constitute a well-known mammalian cell model. They are traditionally used for in vitro investigations related to genetics, toxicity screening and gene expression. The used concentration in this experiment was  $10^8$  cells/ml. For the first measurement both channels are filled with water. In the next measurement channel 1 is filled with a cell suspension of CHO cells whereas channel 2 is only filled with the host medium. For measurement 3 these fillings are exchanged. The subsequent data is self explaining. This example demonstrates that the sensor is capable to detect the filling conditions of the channels and error values as expected from previous calculations could be achieved. However, repetition of loading profiles and longer tests reveal that additional effects deteriorate the achievable accuracy: evaporation of the channel liquids, incomplete filling of the channels and drift effects with currently unknown origin. An example for this is visible in measurement 6 which reveals problems with a repeated dielectric loading situation. For the

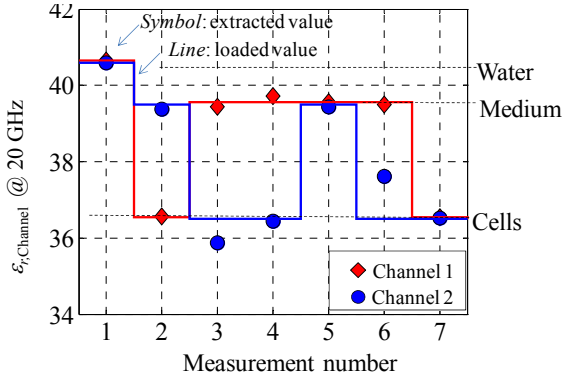


Fig. 6. Extraction results for different loading scenarios. Symbols refer to extracted data, lines to imprinted pattern

resulting extraction error a value of 1.5 (4.1%) is observed which is very different from a simulated value of 0.25 (0.7%) as expected from the calibration with  $m10$ . The extracted relative dielectric constant of the cell solution can be determined to  $\epsilon_{r,Cell} = 36.5 \pm 1.5$ .

The results for a similar test, but with varying cell concentrations  $C_n$  are depicted in Fig. 7.  $C_1$  refers to the previously used concentration of  $10^8$  cells/ml.  $C_2$  has half of the cells of  $C_1$  and  $C_3$  has half of the cells of  $C_2$ . The black lines represent the mean value of the two extraction approaches following equations (1) and (2). The blue boxes show the data range based on the previously determined measurement accuracy. Although there is a non-negligible error, the tendency between extracted dielectric property and cell concentration is visible – also for measurements 8 and 9, where dead cells have been filled into channel 2.

The four-channel device was tested as well. With this device it was possible to clearly detect a change in one channel similar to the simulated calibration measurements from Fig. 4. However, the determination of complex dielectric loading schemes of the channels, similar to the test shown in Fig. 6 and Fig. 7, was problematic. We assume the problem to originate from similar accuracy problems as observed with the two-channel device, but now multiplied with the higher number of channels.

## VI. CONCLUSION

The paper presents a microwave sensor concept which allows for the parallelization of dielectric measurements in a microfluidic channel array at microwaves with only one RF port. For every channel a capacitor is electromagnetically coupled to a microfluidic channel and acts as a transducer. The transducers are part of a CRLH TL whose input impedance is influenced by the dielectric loading situation of the channels. It can be reconstructed by the analysis of the poles and zeros of the input impedance of the sensor circuit. Demonstrators with one, two and four channels have been fabricated, which work in the frequency range between 20 GHz and 25 GHz. They have been tested with water, water-ethanol mixtures and Chinese Hamster Ovary cells and an extraction accuracy for the relative dielectric constant of  $\pm 1.5$  ( $\pm 4.1\%$ ) is obtained. In

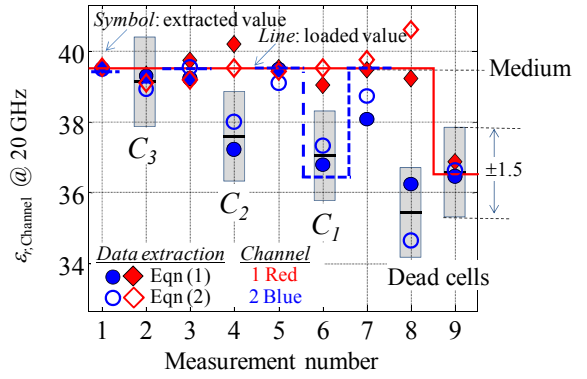


Fig. 7. Extraction results for different loading scenarios with varying cell concentration.

summary the fundamental functionality was demonstrated. However, the tests revealed necessary improvements for the stability of the sensor and the accuracy of the extraction. Hence, next steps will be the improvement of the technological process and a redesign of the structures towards a larger number of measurement channels.

## REFERENCES

- [1] M. Y. Jaffrin and H. Morel, "Body fluid volumes measurements by impedance: A review of bioimpedance spectroscopy (BIS) and bioimpedance analysis (BIA) methods," *Medical Engineering & Physics*, vol. 30, pp. 1257-1269, 12// 2008.
- [2] Y. Zou and Z. Guo, "A review of electrical impedance techniques for breast cancer detection," *Medical Engineering & Physics*, vol. 25, pp. 79-90, 3// 2003.
- [3] A. Bogomolova, E. Komarova, K. Reber, T. Gerasimov, O. Yavuz, S. Bhatt, *et al.*, "Challenges of Electrochemical Impedance Spectroscopy in Protein Biosensing," *Analytical Chemistry*, vol. 81, pp. 3944-3949, 2009/05/15 2009.
- [4] K. Cheung, S. Gawad, and P. Renaud, "Impedance spectroscopy flow cytometry: On-chip label-free cell differentiation," *Cytometry Part A*, vol. 65A, pp. 124-132, 2005.
- [5] C. Dalmay, A. Pothier, P. Blondy, F. Lalloue, and M.-O. Jauberteau, "Label free biosensors for human cell characterization using radio and microwave frequencies," in *Microwave Symposium Digest, 2008 IEEE MTT-S International*, 2008, pp. 911-914.
- [6] K. Grenier, D. Dubuc, P.-E. Poleni, M. Kumemura, H. Toshiyoshi, T. Fujii, *et al.*, "Integrated broadband microwave and microfluidic sensor dedicated to bioengineering," *Microwave Theory and Techniques, IEEE Transactions on*, vol. 57, pp. 3246-3253, 2009.
- [7] T. Chen, F. Artis, D. Dubuc, J. J. Fournie, M. Poupot, and K. Grenier, "Microwave biosensor dedicated to the dielectric spectroscopy of a single alive biological cell in its culture medium," in *Microwave Symposium Digest (IMS), 2013 IEEE MTT-S International*, 2013, pp. 1-4.
- [8] H. Morgan, T. Sun, D. Holmes, S. Gawad, and N. G. Green, "Single cell dielectric spectroscopy," *Journal of Physics D: Applied Physics*, vol. 40, p. 61, 2007.
- [9] M. Schübler, M. Puentes, D. Dubuc, K. Grenier, and R. Jakoby, "Simultaneous dielectric monitoring of microfluidic channels at microwaves utilizing a metamaterial transmission line structure," in *Engineering in Medicine and Biology Society (EMBC), 2012 Annual International Conference of the IEEE*, 2012, pp. 6273-6276.
- [10] M. Schübler, M. Puentes, C. Mandel, and R. Jakoby, "Multi-resonant perturbation method for capacitive sensing with composite right/left-handed transmission lines," in *Microwave Symposium Digest (MTT), 2010 IEEE MTT-S International*, 2010, pp. 481-484.
- [11] M. Schübler, M. Puentes, C. Mandel, and R. Jakoby, "Capacitive level sensor for layered fillings in tanks and vessels based on metamaterial transmission line," in *Sensors, 2011 IEEE*, 2011, pp. 1966-1969.